



Published in final edited form as:

J Control Release. 2017 June 10; 255: 36–44. doi:10.1016/j.jconrel.2017.03.397.

BCG Vaccine Powder-Laden and Dissolvable Microneedle Arrays for Lesion-Free Vaccination

Fan Chen^{a,b}, Qinying Yan^{a,c}, Yang Yu^a, and MeiX. Wu^{a,*}

^aWellman Center for Photomedicine, Massachusetts General Hospital (MGH), Department of Dermatology, Harvard Medical School (HMS), Boston, Massachusetts 02114, USA.

^bHubei Collaborative Innovation Center for Green Transformation of Bio-Resources, Life Sciences School of Hubei University, 368 Youyi Road, Wuhan 430062, China.

^cCollege of Pharmaceutical Sciences, Zhejiang University of Technology, 18 Chaowang Road, Hangzhou 310032 China.

Abstract

Live attenuated Bacille Calmette-Guerin (BCG) bacillus is the only licensed vaccine for tuberculosis prevention worldwide to date. It must be delivered intradermally to be effective, which causes severe skin inflammation and sometimes, permanent scars. To minimize the side effects, we developed a novel microneedle array (MNA) that could deliver live attenuated freeze-dried BCG powder into the epidermis in a painless, lesion-free, and self-applicable fashion. The MNA was fabricated with biocompatible and dissolvable hyaluronic acid with a deep cave formed in the basal portion of each microneedle, into which BCG powder could be packaged directly. Viability of BCG vaccine packaged in the caves and the mechanical strength of the powder-laden MNA did not alter significantly before and after more than two months of storage at room temperature. Following insertion of the MNA into the skin, the individual microneedle shafts melted away by interstitial fluid from the epidermis and upper dermis, exposing the powder to epidermal tissues. The powder sucked interstitial fluid, dissolved slowly, and diffused into the epidermis in a day against the interstitial fluid influx. Vaccination with BCG-MNA caused no overt skin irritation, in marked contrast to intradermal vaccination that provoked severe inflammation and bruise. While causing little skin irritation, vaccination efficacy of BCG-MNAs was comparable to that of intradermal immunization whether it was evaluated by humoral or cellular immunity. This powder-laden and dissolvable MNA represents a novel technology to sufficiently deliver live attenuated vaccine powders into the skin.

*Correspondence and requests for materials should be addressed to M.X.W. (mwu5@mgh.harvard.edu).

Conflict of Interest

Authors declare no conflict of interest.

Publisher's Disclaimer: This is a PDF file of an unedited manuscript that has been accepted for publication. As a service to our customers we are providing this early version of the manuscript. The manuscript will undergo copyediting, typesetting, and review of the resulting proof before it is published in its final citable form. Please note that during the production process errors may be discovered which could affect the content, and all legal disclaimers that apply to the journal pertain.

Keywords

BCG powder; microneedles; lesion-free; skin delivery

1. Introduction

Tuberculosis (TB) is caused by *Mycobacterium tuberculosis* (*M.tb*) and continues to be a leading cause of mortality among bacterial diseases. Although major progress has been made towards the global reduction of TB, TB still killed 1.5 million people and 9.6 million new TB cases were estimated in 2014 alone [1]. Approximately one-third of the world's population is currently infected with *M.tb* and about 5% of these infected people may progress to active disease during their lifetime. The risk of reactivating the infection and the resultant mortality are significantly escalated in HIV-infected individuals. This, along with emergence of multi-drug resistant strains [2,3], complicates this already miserable situation and raises an urgent need for an efficacious vaccine against TB. The Bacille Calmette-Guérin (BCG) vaccine, first introduced in 1921, remains to be the only licensed vaccine for TB prevention [4]. A great deal of efforts have been devoted to the development of a new vaccine against TB in the past two decades, but no any substitute or booster over the BCG vaccine has been developed so far [5]. A recent failure of a clinical trial of a new TB vaccine named MVA85A to enhance efficacy of the BCG vaccine in South African infants reaffirms the challenges we are facing to improve BCG-induced immune protection [6]. Alternatively, TB epidemics can be better controlled by broadening BCG vaccination coverage in neonates before they are exposed to any infection [7]. Development of a pain-less, lesion-free, self-applicable, and cost-effective vaccination approach would undeniably facilitate this alternative strategy in mass neonatal vaccination in developing countries.

BCG vaccine is currently administered intradermally to newborns or neonates using a hypodermic needle. It requires skilled healthcare professionals and it is often unreliable [8–10]. If the vaccine is accidentally given subcutaneously, which occurs ~5%, the bacillus may infect local tissues and the infection can spread to the regional lymph nodes, causing either suppurative or nonsuppurative lymphadenitis [11,12]. Hence, intradermal (ID) immunization of BCG vaccine poses a real risk to both vaccinees and healthcare providers. Moreover, the skin vaccination is well known to cause pain, accidental needle stick injuries, serious skin inflammation, and scars. These adverse events discourage children and parents, leading to a high level of non-compliance [11,13]. Microneedle arrays (MNAs) were investigated for delivering BCG vaccines in which the vaccine was coated onto a metal MNA but its viability lost more than 50% in the absence of preservatives or surfactant or 25% in the presence of trehalose and surfactant after storage for only 7 days at 25°C [14]. Dissolving MNAs were next engineered to encapsulate and deliver bioactive molecules and vaccines [15–18], all of which however required a mixture of the bioactive molecules with monopolymer prior to polymerization. The polymerization process often compromises the activity or immunogenicity of the bioactive materials considerably, which are not suitable to live attenuated BCG bacilli.

Currently BCG vaccine is freeze-dried powder and sealed under vacuum in a glass ampoule. The powder has to be diluted with saline water and injected within hrs, which often incurs errors owing to inappropriate opening of the glass ampoule and mishandling of the reconstitution. To eliminate the reconstitution procedure and minimize skin irritation, we explored a micro-fractional delivery of powdered vaccines into the skin, in which an array of self-healing microchannels were generated in the epidermis and upper dermis by ablative fractional laser, followed by topical application of powdered vaccine-coated array patches [19,20]. While greatly promoted of powder vaccines into the skin, the laser-perforated skin showed little reactogenicity. However, laser was required to perforate the skin and powdered vaccines fractionally coated in the patch must be aligned precisely with the individual microchannels on the skin for a high efficiency of delivery. These drawbacks are overcome by our newly engineered dissolvable, powder-laden MNAs as presented in the current study. The novel MNA could efficiently deliver powdered BCG vaccines and elicit innate, humoral, and cellular immunity similarly as traditional ID vaccination, while causing little skin irritation. The MNA could be stored for more than 60 days at room temperature without adverse effects on the penetration ability of the MNA or viability of the BCG vaccine.

2. Materials and methods

2.1 Mycobacteria and animals

Mycobacterium bovis BCG strain (Danish 1331) was purchased from American type culture collection and expanded as per manufacturer's instructions (ATCC-35733). For powder preparation, the *Mycobacterium* was grown at 37°C to a mid-log phase in BBL™ Mycoflasic Middlebrook 7H9 broth with 0.2% glycerol from the Becton, Dickinson and Company (BD). Colony forming units (CFU) were enumerated after a series of 10-fold dilutions and culturing the diluted bacilli on BBL™ Middlebrook and Cohn 7H10 agar plates supplemented with 0.5% glycerol (BD). Inbred BALB/c and C57BL/6 mice at 5 weeks of age were purchased from Charles River Laboratories and both genders were used randomly with no notable difference. The animals were housed in the specific pathogen-free animal facilities of Massachusetts General Hospital (MGH) in compliance with institutional, hospital and NIH guidelines. All studies were reviewed and approved by the MGH Institutional Animal Care and Use Committee.

2.2 Fabrication of BCG powder-laden, dissolvable MNAs

MNAs were fabricated via micromolding technologies as described with some modifications [21]. In brief a female polydimethylsiloxane (PDMS, Dow Corning) mold was used to fabricate a 6 × 9 array of microneedles each in a height of 200 μm and a base diameter of 100 μm. A 20% sodium hyaluronate (HA) (750~1000 kDa from Lifecore) solution in distilled water was added into the female PDMS mold mounted in a 6-well plate followed by centrifugation for 5 min at 1500 rpm/min at 4°C twice with the plate rotated horizontally at 90° following each centrifugation. The plate was centrifuged for 5 min at 3000rpm/min twice again as above to make sure that each cavity of the female MNA mold was evenly filled with HA and no bubbles were formed in the gel. Excess HA was removed gently and flatly using a cotton swab without disturbing HA microneedles in the cavity of the negative

MNA mold. HA was polymerized in a negative pressure container at room temperature for overnight, forming a cave at the upper portion of each microneedle at 25~30 μm in depth.

To prepare BCG powder, bacilli at a mid-log growth phase were collected, washed three times, re-suspended with PBS, and lyophilized at -40°C . The powdered BCG vaccine was ground to make them more homogeneous before adding into the base of the MNA. The plate was centrifuged for 10 min at 3000rpm/min at 4°C twice with the plate rotated horizontally at 90° following each centrifugation. The process was repeated two to three times until all microneedles in the array were fully laden. Additional HA solution at 15% was added to cover the MNA at ~ 0.5 mm in thickness, followed by centrifugation at 3000 rpm/min for 10 min twice with 90° rotation in between. The plate was dried in a negative pressure container overnight at room temperature. The resultant BCG-MNA was peeled off by a transparent adhesive tape. As a control, MNA without powder was prepared similarly as empty MNA. To visualize the powder packed within microneedles, powdered Alexa fluor 555-ovalbumin (OVA) (Molecular Probes) was added to the hollow of the microneedles in place of BCG, whereas HA solution mixed with a small amount of fluorescein isothiocyanate (FITC, Sigma) was used to fabricate the cave MNA as above. The resultant MNA was scanned by two photon confocal microscopy.

2.3 Quantification and viability of encapsulated BCG vaccine

To quantify BCG vaccine encapsulated in each microneedle in the array, we first established a standard curve by mixing sulforhodamine B (SRB) powder with BCG vaccine powder at a 1: 4 ratio by weight in dH_2O , followed by measurement of SRB fluorescent density on SpectraMax®, Molecular devices, USA. The amount of BCG vaccine powder was correlated linearly with SRB absorbance at 640 nm. The experiment was repeated for three times with 6 MNAs in each experiment. To evaluate viability of the BCG vaccine encapsulated within the MNA before and after storage at room temperature in a dark and dry desiccator, a portion of the MNA consisting of 24 microneedles was cut for each test at indicated days of storage and dissolved in 1ml PBS, followed by a series of ten-fold dilution. The diluted and reconstituted BCG vaccine of 100 μl from each sample was inoculated onto 7H10 agar dishes and cultured for 30 days at 37°C . Bacterial colonies of the reconstituted BCG vaccine from 24 microneedles in the agar dishes were counted manually in a sample-blind fashion. The result was expressed as an average CFU number of BCG vaccine powder per 24 microneedles.

2.4 Immunizations and skin reaction observation

BALB/c mice were anesthetized by intramuscular injection of ketamine at 100mg/kg and xylazine at 10mg/kg followed by hair removal on the lower dorsal skin with an animal hair clipper and depilatory cream. The mice were randomly divided into four groups with six in each and immunized by BCG vaccine with MNA or ID injection at a dose of 6 μg BCG per mouse. Control mice were mock immunized with empty MNA or PBS, respectively. Only a portion of a MNA containing 24 microneedles was used to immunize each mouse. The MNA was inserted into the skin by pressing it firmly with a thumb and removed after 15 min of the application. The inoculation sites were photographed daily for 10 days post-immunization to track skin reaction. Skin temperature was also monitored daily by an

infrared thermometer (LA CROSSE) for 10 days at the sites of inoculation as well as a distant skin area of the same mouse as references. The differences in the skin temperature of the two sites in the same mouse were recorded as a temperature change over time.

2.5 Histology and images of the vaccination site

Mice were immunized as above and sacrificed on day 3 after the immunization to examine skin inflammation at the sites of vaccination. The skins of inoculation sites about 1cm² in size were dissected at indicated days, fixed, and stained by a standard haematoxylin and eosin (H&E) procedure. The slides were scanned and analysed by NanoZoomer (Hamamatsu). To visualize non-overlapping skin reaction among different micropores generated by MNA, MHC II-EGFP C57BL/6 mice that expressed MHC class II molecule infused into enhanced green fluorescent protein (GFP) were used. The ear of the mice was inserted with BCG-MNA as above and examined 6 hr later by two photon confocal microscopy.

2.6 Intracellular cytokine productions

Small blood samples were collected from the orbital sinus of mice for evaluating immune responses elicited by BCG vaccines overtime. Peripheral cells were isolated by centrifugation after lysis of red blood cells with ACK buffer and cultured in DMEM medium (Sigma) supplemented with 10% fetal calf serum (FCS), 100 U/ml penicillin, and 100 mg/ml streptomycin (Gibco). NK cells were analyzed in one week and T cells in four weeks post-immunization by stimulating the cells for 16 hours with a pool of antigen stimulants each at a final concentration of 2 pg/ml for all assays. The antigens used were three immunogenic mycobacterial proteins (ESAT-6, Ag85, CFP-10) and 16 peptides (TB 10.4) and all obtained from BEI Resource, NIH. The cells were continuously cultured for another 5 hr in the presence of Golgiplug (BD) per the manufacturer's instruction. The activated cells were surface stained with PE-anti-CD49B (Invitrogen), FITC-anti-CD4 or Percp-cy5.5-anti-CD8 antibody. The stained cells were permeabilized with a Cytotfix/Cytoperm buffer (BD Biosciences), followed by intracellular staining with PE-anti-IFN- γ , PE-cy7-anti-IL-2 or APC-anti-TNF- α antibody, all from BD Biosciences. The numbers of specific cell types were quantified by a FACS Aria (BD) and analysed using FlowJo software (version 7.6.5, OR, USA).

2.7 Detection of BCG specific Antibodies

Vaccine-specific IgG, IgG1, and IgG2a were measured by an enzyme-linked immunosorbent assay (ELISA) using BCG bacillus outer membrane extract as coating antigens [22,23]. The outer membrane extract was prepared by suspension of the bacilli for 1 hour in a buffer solution (30 mM Tris, 2 mM EDTA, pH 8.5) in the presence of sodium deoxycholate [10 % (w/v)] at a rate of 0.1–0.25 ml/g biomass. After centrifugation, the supernatant was collected and ultracentrifuged at 70,000g for 4 hrs at 4°C (Beckman Coulter) to obtain the outer membrane extract. The extract was re-suspended in PBS, passed through firstly a 0.45 μ m Sartorius Minisart-plus filter, and then a 0.22 μ m filter. The resultant outer membrane extract was stored at 4°C and used at a concentration of 1 pg/mL to coat ELISA plates overnight in NaHCO₃ buffer, pH9.6. The plates were incubated for 2 hr with serum samples at 1:32 dilution, after which HRP-conjugated goat anti-mouse IgG (NA931V, GE healthcare,

dilution 1:6,000), IgG1 (A90–105P, Bethyl, dilution 1:10,000), or IgG2a (61–0220, Life Technologies, dilution 1:2,000) was added to each well and incubated for 1 hr. The assay was developed by o-phenylenediamine dihydrochloride-FLCU substrate solution (Sigma-Aldrich) followed by measurement of the colored reaction at 490 nm using microplate ELISA reader (SpectraMax®, Molecular devices, CA, USA).

2.8 Cytokine production in lymphocytes in the lungs and spleens

Lung and spleen were dissected from indicated mice after 90 days of immunization and finely minced. The minced lung tissue was suspended in 25 ml DMEM medium plus 150 U/ml Collagenase I (Gibco) and 10U/ml DNase II (Sigma) and digested for one hour at 37°C with shaking at 200 rpm. After removal of red blood cells by ACK buffer, the digested lung tissue was pressed through a 40µm cell strainer to obtain single cell suspension. The spleen was forced directly through a 70 µm cell strainer, without digestion, to obtain single cell suspension after mincing. The single cell suspensions prepared from lung or spleen were stimulated at 37°C with 5% CO₂ for 72 hr by a pool of BCG specific stimulants as above in DMEM medium (Sigma, UK) supplemented with 10% FCS and antibiotics (100 U/ml penicillin and 100 mg/ml streptomycin) at a cell density of 2×10⁶/ml. Productions of TNF-α, IL-6, IL-12 and IL-17 in the supernatants were measured by corresponding ELISA kits (eBiosciences) according to manufacturer's instructions [24,25],

2.9 Statistical analysis

The data were analyzed by one-way ANOVA among multiple groups or a Student's t-test between two groups with Prism Graph Pad software (Graph-Pad Software, La Jolla, C A, USA). Mycobacterial counts were log₁₀ transformed and analyzed using the unpaired Student's t-test. A p value < 0.05 was considered significant.

3. RESULTS

3.1 Fabrication of dissolvable and powder-laden MNAs

MNAs were made up with biocompatible and dissolvable HA in a female PDMS mold with some modifications [21,26]. A deep cave developed in the base of each microneedle (Figure 1 A & B) as a consequence of polymer condensation during polymerization [27]. To better visualize the cave, HA was mixed with a trace amount of FITC prior to polymerization and the resultant MNA was imaged by confocal microscopy (Figure 1C). The caves of the MNA were then filled with powdered OVA conjugated with a red fluorescent dye Alexa fluor 555 (Figure 1C). When inserted into the skin, shafts of the MNA melted away in 10–15 min, exposing the powder to the epidermis (Figure 1D, 2hr). The powder sucked interstitial fluids from the skin tissue, dissolved slowly, and diffused into the epidermis over time against the interstitial fluid influx similarly to the powder drained into laser-generated microchannels previously demonstrated [19,20,28]. The powder was spreading horizontally into the epidermis and then vertically into the upper dermis (Figure 1D). Most powder entered the skin tissue in 19 hr as suggested by a hollow at the center of the powder delivery site (Figure 1D, the lower right corner). Entrance of the powder into the skin was clearly seen in 6 hr after MNA insertion into the ear of MHC II-GFP mice in a 3D image where powder was embedded within and passed through Langerhans cell-enriched epidermis (Figure 1E,

upper). A top view of the powder delivery was collected 15 min after removal of the OVA-MNA (Figure 1E, lower) showing the powder and GFP⁺ Langerhans cells on the same level, in agreement with the powder deposited within the skin. The powdered BCG vaccine appeared to actively attract MHC-II⁺ cells as suggested by surrounding each microneedle-generated pore with a large number of cells expressing GFP (Figure 1F). The heavily concentrated GFP⁺ cells around each pore explain the dense GFP fluorescence in the epidermic layer in Figure 1E, upper. We intentionally designed the MNA at a sufficient distance of 4 x bases between any two microneedles to prevent overlap of skin reactivity caused by a microneedle nearby (Figure 1F). By doing so, BCG-induced inflammation could be well constrained around each microneedle and quickly resolved, giving rise to lesion-free skin vaccination [29].

3.2 Loading capacity and storage of the MNA

The peak of light absorbance of the mixture was 640 nm, which was shifted slightly from the known SRB absorbance of 560 nm probably owing to absorbance of or binding to BCG bacilli, although a further study is required to clarify it. The amount of SRB was proportionally correlated with the amount of BCG vaccine powder with a coefficient of determination $R^2 = 0.996$ (Figure 2A). The average of BCG vaccine per microneedle was about 0.25 μg from a total of 9 microneedles in 6 different patches with 95% CI (Figure 2B). Similar results were obtained from three independent experiments each with 6 MNAs analyzed (Figure. 2B). In other words, approximate 13.5 μg of BCG powder could be loaded per a single patch on average. In addition to a high loading capacity, viability of BCG vaccine encapsulated in the MNA was little altered before and after loading and during 60 days of storage at room temperature. Although the CFU log value was decreased by about 7% in 90 days of storage (Figure 2C), it was without statistical significance. The decrease was probably associated with an intrinsic viability of the BCG powder that is conventionally stored at 4°C. The 90 days of storage did not diminish the mechanical strengths of the MNA either. The MNA could be pierced through the mouse epidermis as similarly as the one freshly made (Figure 2D) and microneedles-mediated perforation of skin was confirmed histologically, showing the skin being pierced effectively (Figure 2E). The results suggest that the BCG powder-laden MNA is great not only for BCG delivery but also for BCG vaccine storage.

3.3 Skin reaction after inoculation

It is well known that BCG vaccination causes severe skin inflammation and permanent scars sometimes. All these adverse events were completely averted by vaccination with BCG-MNA. The inoculation site for BCG-MNA was indistinguishable from the normal skin 1 day after immunization (Figure 3A, the second panel). The micropores generated by either BCG-MNA or empty MNA were evidenced similarly within 6 hr after insertion but no longer seen in 24hr. In accordance with this, the micropores in the skin generated by individual microneedles of the MNA were not recognizable in the histological studies after 3 days even with 50X enlargement (Figure. 3B, the second panel). In sharp contrast, ID injection caused stye and bruise which did not disappear for 10 days (Figure 3A, the first panel). Similar skin reaction including a stye and erythema was also observed at the site of PBS injection on day 1, though waning completely on day 3 (Figure 3A). The severe inflammation was clearly

evidenced by the large lesion full of inflammatory cells at the site of ID injection (Figure 3B, the first panel). The results confirm that the MNA can delivery BCG powder into the skin without provoking overt skin inflammation. The local skin temperature, another indicator of skin inflammation, was also monitored daily during the experimental period. Skin temperature of ID group significantly increased from day 2 to day 8 after immunization when compared to all other groups, in agreement with serious skin inflammation (Figure 3C). Although the skin temperature was also elevated slightly in the first four days of BCG-MNA application, it was without a statistical difference compared to mice receiving either empty MNA or PBS ID administered. The data corroborate inflammation-blunt, lesion-free delivery of BCG vaccine into the skin.

3.4 Cellular and humoral immune responses induced by BCG-MNA

Because of a high loading capacity of the MNA, we used only a portion of the MNA consisting of 24 BCG-packed microneedles with a total of 6 μg BCG vaccine powder per mouse for immunization. BCG antigens-specific activation of peripheral natural killer (NK) cells was examined one week after immunization by anti-CD49B antibody and antigens-induced production of anti-IL-2 or TNF- α cytokine. NK cells have been recently suggested to participate in adaptive innate immunity or “trained immunity” following BCG vaccination [30], IL-2 may contribute to the expansion of NK cells and aid immune responses to BCG [31]. TNF- α is essential for protection against *M.tb* infection [32], The number of CD49B⁺IL-2⁺ cells was elevated in circulation significantly in mice immunized by BCG-MNAs when compared to mice receiving PBS or empty MNAs (Figure 4A), which were comparable to that of ID vaccination. NK cells producing TNF- α were found no significant differences irrespective of the vaccination procedures or whether BCG was given (Figure 4B). We went on to study T cell activation in the mice four weeks after immunization by assessing antigen-specific induction of IFN- γ and TNF- α expression in T cells isolated from blood samples, two cytokines important to clean intracellular pathogens. IFN- γ ⁺ CD4⁺T cells (Figure 4C) and IFN- γ ⁺ CD8⁺ cells (Figure 4D) were all significantly increased to a similar degree in mice receiving BCG vaccine regardless of whether it was delivered by ID or MNA over corresponding mock immunizations. The similar increases were also seen with TNF- α ⁺ CD4⁺ cells in both ID and BCG-MNA groups (Figure 4E). Different from CD4⁺TNF- α ⁺ T cells, there was no significant difference in the number of CD8⁺T cells producing TNF- α among the four groups (Figure 4F). The results suggest that BCG-MNA vaccination is similar to ID immunization in activation of T and NK cells.

Apart from cellular immune responses, we also analyzed humoral immunity in the mice four weeks after immunization, because antibodies have been shown to have significant impact on the immune responses against TB [33,34], In comparison with mice receiving empty MNA and PBS, the amounts of IgG1 (Figure 5B) and IgG2a (Figure 5C) antibodies were increased significantly in the presence vs. the absence of BCG vaccines with more predominant effect on IgG1. Efficacy of BCG-MNA vaccination in stimulation of IgG1 and IgG2a seems comparable to ID vaccination (Figure 5). However, while total IgG response was significantly higher in mice receiving BCG intradermally in comparison with control groups mock immunized by empty MN or PBS (Figure 5A), the increase in the total IgG in BCG-MN group was not significant. Whether epidermic immunization may favor T and NK

cell immune responses (Figure 4 A to D) but not humoral immune responses (Figure 5) is under current investigation.

3.5 Various cytokine productions in the spleens and lungs

To further corroborate similar efficacy of these two immunization approaches, cytokines including TNF- α , IL-6, IL-12, and IL-17 were measured in the lung and spleens in 90 days of the immunization. TNF- α is required to sustain protective immunity against *M.tb* infection although it alone is insufficient [32], while IL-6 and IL-12 are crucial for the differentiation of protective Th1 cells in light of increasing IFN- γ -producing T cells observed after BCG vaccination (Figure. 4)[35]. IL-17 induces direct bacterial killing by macrophages [36,37] and is involved in defense against intracellular pathogens[38]. Lymphocytes in both spleen and lung apparently produced significantly higher levels of all these four cytokines in the presence of BCG vaccine than in the absence of the vaccines irrespective of the vaccination procedure (Figure 6), in agreement with similar efficacy of BCG-MNA vaccination with that of ID.

4. DISCUSSION

A majority of vaccines, with only a few exceptions, are administered intramuscularly despite the fact that the muscle is inferior to the skin for stimulating immune responses. Among the few exceptions, BCG vaccine is the one that must be given to the skin to be efficacious even though it is inconvenience and with a high rate of adverse events. The current BCG vaccine is provided as freeze-dried powder and shipped along with a dilute in two ampoules for each dose of the vaccine. Reconstitution of the powdered BCG vaccine with a dilute is required before ID injection because the live attenuated bacilli cannot be stored in a liquid form. Liquid form of the vaccine is unstable and prone to contamination and cannot be frozen, which creates additional error-prone procedures in association with reconstitution, apart from requiring disposal of sharp biohazardous needles and increased burden of transportation. All these issues can be effectively addressed by direct delivery of BCG vaccine powder into the skin as presented in the current study. Secondly, the MNA can be potentially self-applicable and eliminate the need of skilled professional technician. Thirdly, the powdered MNA can be stored for at least 60 days at room temperature, with unaltered mechanical strengths of the microneedles and well sustained viability of the bacilli. The long shelf-life is extremely valuable to the resource desert areas where cold chain storage and transportation are impossible but the vaccine is mostly needed. Finally and most importantly, the BCG-MNA displays similar vaccination efficacy without incurring significant skin inflammation, in marked contrast to ID vaccination that causes severe inflammation for weeks at the inoculation site.

Moreover, this dissolvable, powder-loadable MNA can be loaded with many powdered vaccines or drugs with no need of modifying the MNA fabrication procedure. The novel MNA would thus have broad applications in skin delivery of various drugs or vaccines besides BCG. Currently, several types of MNAs, including hollow MNAs for delivering liquid forms of vaccines or drugs and two types of solid MNAs, have been extensively described for skin delivery [39-47]. The solid MNAs can be coated with vaccines or drugs on

the surface of each microneedle or the vaccines and drugs can be embedded in each microneedle by mixing the vaccine with monopolymer before polymerization. For either solid MNA, the MNA has to be optimized and fabricated in a drug or vaccine-specific manner. For instance, excipients, stabilizers, and polymerization or coating conditions are optimized for best preservation of influenza vaccines in fabrication of dissolvable or coating MNA. These optimal conditions are likely very different from those required to best protect BCG vaccine and must be tested individually. On the contrary, our powder-loadable MNA is universal for many vaccines or drugs as long as they can be produced in a form of powder, which can simplify the manufacture's practice and reduce the cost of MNA fabrication considerably. In general, powdered vaccines or drugs are more stable against degradation and chemical modification. Various technologies are also available to transform liquid vaccines, biological agents or drugs into dry forms, like freeze-drying, spray-drying, and spray-freeze-drying. The powder-laden MNA may be applicable to diphtheria, tetanus, malaria [48], anthrax and staphylococcal toxic shock vaccines as well since these vaccines can elicit effective immune responses when delivered by other microneedles [49].

The powder packaged in the MNA was first hydrated and dissolved by interstitial fluids after shafts of the microneedles melted away, followed by diffusion into the epidermis against the interstitial fluid influx. The powder would not spread onto the skin surface owing to a lack of fluid. Deposition of all the powder into the skin is not necessary for efficient delivery of the powder by powder-laden MNA, because the powder can be drained into the skin by the interstitial fluid influx. In this regard, our recent study demonstrated that powdered substance fractionally coated on a patch could sufficiently enter the skin even if the powder-coated patch was topically placed on a perforated skin [28]. The unique property of powder being drained into the skin by the interstitial fluid can thus permit a delivery of a high amount of vaccines or drugs via MNA, for instance, by extension of the basal cave above the skin as shown in our recent publication [28], which scores another advantage over traditional dissolvable and vaccine-coated MNAs. In addition, the powder was gradually spreading into the epidermis and upper dermis, minimizing their leakage into the circulation. This controllable delivery is crucial for BCG vaccine to prevent unwanted infections of other tissues by the bacterium and to ensure the safety of the vaccination. This predominant epidermic delivery is also a key to allergen administration in immunotherapy of allergy to prevent anaphylaxis [20]. In comparison with delivery of powdered vaccines via laser-perforated skin [19,20], the current technology represents a saltation improvement because no laser treatment is required in the current delivery system.

Our investigation concluded that BCG-powder MNAs elicited comparable immune responses as those induced by traditional ID vaccination whether the immune responses were evaluated by NK and T cell activation and cytokine production in the lungs and spleens. The efficacy of BCG-MNA vaccination might be underestimated because BCG-MNA was removed after applied into the skin for only 15 min. Resident BCG powder might be presented in the base of the MNA, resulting in a delivery of less than 6 pg per mouse, which was not factored into the results. Extension of the application to 1 hr should further improve the efficacy. Currently, there are no established correlates of specific immune responses with protection efficacy of the BCG vaccine. A challenge study is required in the future to confirm similar protections between the two immunization methods, which are

restricted to the animal facility with a BSL-3 safety standard. NK cells may contribute to the non-specific (heterologous) benefits of BCG vaccination [30]. The cells are activated by BCG vaccine non-specifically after re-stimulation as evidenced by increasing expressing IL-2 in mice immunized with BCG vaccine but not after mock immunization [50]. Likewise, peripheral CD4⁺T cells produced more IFN- γ and TNF- α after BCG vaccination and these two cytokines are important in control of *M.tb* infection[51,52]. While peripheral CD8⁺cells also generated more IFN- γ in response to BCG vaccine, the cells did not produce more TNF- α under similar vaccination. These data demonstrate that BCG-MNA vaccination can stimulate strong cellular immunity at least as efficiently as ID vaccination, arguing strongly for its potential in place of traditional ID injection.

5. Conclusion

Many vaccines or drugs are currently prepared in a form of powder owing to stronger stability and longer shelf-life than a liquid form of these substances. However, powder vaccines or drugs require reconstitution with a solution prior to injection, a procedure that is inconvenience and error-prone. The powder-laden dissolvable MNA can deliver powders directly into the skin in a minimal invasive, needle-free, and painless fashion, conferring great advantages over ID injection.

Acknowledgment

We thank the Wellman Photopathology Core for their help in histology and flow cytometry analyses during this project and Drs. Ji Wang and Bo Li for their assistance in MNA preparation and imaging studies, respectively. This work is supported in part by the National Institutes of Health Grants AI089779 and AI13458 and department funds to M.X.W.

REFERENCES:

1. World Health Organization. Global tuberculosis report 2015.
2. Günther G , Multidrug-resistant and extensively drug-resistant tuberculosis: a review of current concepts and future challenges. *Clin. Med.* 14(2014)279–285.
3. Cohen T , Lipsitch M , Walensky RP , Murray M , Beneficial and perverse effects of isoniazid preventive therapy for latent tuberculosis infection in HIV-tuberculosis coinfecting populations. *Proc. Natl. Acad. Sci. USA* 103(2006)7042–7047.16632605
4. Calmette A , Preventive vaccination against tuberculosis with BCG. *Proc. R. Soc. Med.* 24(1931)1481–1490.19988326
5. Principi N , Esposito S , The present and future of tuberculosis vaccinations. *Tuberculosis* 95 (2015)6–13.25458613
6. Tameris MD , Hatherill M , Landry BS , Scriba TJ , Snowden MA , Lockhart S , Shea JE , McClain JB , Hussey GD , Hanekom WA , Mahomed H , McShane H , MVA85A020 Trial Study Team, MVA85A020 Trial Study Team. Safety and efficacy of MVA85 A, a new tuberculosis vaccine, in infants previously vaccinated with BCG: a randomised, placebo-controlled phase 2b trial. *Lancet* 381 (2013)1021–1028.23391465
7. Me Shane H , Understanding BCG is the key to improving it. *Clin. Infect. Dis.* 58 (2014) 481–482.24336910
8. Hawkrige A , Hatherill M , Little F , A Goetz M , Barker L , Mahomed H , Sadoff J , Hanekom W , Geiter L , Hussey G , South African BCG trial team. Efficacy of percutaneous versus intradermal BCG in the prevention of tuberculosis in South African infants: randomised trial. *BMJ* 337(2008)a2052.19008268

9. Flynn PM , Shenep JL , Mao L , Crawford R , Williams BF , Williams BG . Influence of needle gauge in Mantoux skin testing. *Chest* 106(1994)1463–1465.7956403
10. Pasteur MC , Hall DR , The effects of inadvertent intramuscular injection of BCG vaccine. *Scand. J. Infect. Dis.* 33(2001)473–474.
11. Mitragotri S , Immunization without needles. *Nat. Rev. Immunol.* 5(2005)905–916.16239901
12. Jeena PM , K Chhagan M , Topley J , Coovadia HM , Safety of the intradermal Copenhagen 1331 BCG vaccine in neonates in Durban, South Africa. *Bull World Health Organ.* 79(2001)337–343.11357213
13. WHO and UNICEF release first ever. “State of the World’s Vaccines” report. *Indian Pediatr.* 33(1996)978–981.
14. Hiraishi Y , Nandakumar S , Choi SO , Lee JW , Kim YC , Posey JE , Sable SB , Prausnitz MR , Bacillus Calmette-Guérin vaccination using a microneedle patch. *Vaccine* 29(2011) 2626–2636.21277407
15. Ito Y , Yoshimitsu J , Shiroyama K , Sugioka N , Takada K , Self-dissolving microneedles for the percutaneous absorption of EPO in mice. *J. Drug. Target.* 14(2006)255–261.16882545
16. Lee JW , H Park J , Prausnitz MR , Dissolving microneedles for transdermal drug delivery. *Biomaterials* 29(2008)2113–2124.18261792
17. Sullivan SP , Murthy N , Prausnitz MR , Minimally invasive protein delivery with rapidly dissolving microneedles. *Adv. Mater.* 20(2008)933–938.23239904
18. Sullivan SP , Koutsonanos DG , Del Pilar Martin M , Lee JW , Zamitsyn V , Choi SO , Dissolving polymer microneedle patches for influenza vaccination. *Nat. Med.* 16(2010) 915–920.20639891
19. Chen X , Kosiratna G , Zhou C , Manstein D , Wu MX , Micro-fractional epidermal powder delivery for improved skin vaccination. *J. Control. Release.* 192 (2014)310–316.25135790
20. Kumar MN , Zhou C , Wu MX , Laser-facilitated epicutaneous immunotherapy to IgE-mediated allergy. *J. Control. Release.* 235(2016)82–90.27235977
21. Liu S , Jin MN , Quail YS , Kamiyama F , Katsmni FL , Sakane T , Yamamoto A , The development and characteristics of novel microneedle arrays fabricated from hyaluronic acid, and their application in the transdermal delivery of insulin. *J. Control. Release.* 161 (2012) 933–941.22634072
22. Tirado Y , Puig A , Alvarez N , Borrero R , Aguilar A , Camacho F , Reyes F , Fernandez S , Pérez JL , Espinoza DM , A Payán J , Sanniento ME , Norazmi MN , Hernández-Pando R , Acosta A , Protective capacity of proteoliposomes from *Mycobacterium bovis* BCG in a mouse model of tuberculosis. *Human Vaccines & Immunotherapeutics* 11(2015)657–661.25671612
23. Rodriguez L , Tirado Y , Reyes F , Puig A , Kadir R , Borrero R , Fernández S , Reyes G , Alvarez N , Garcia MA , Sanniento ME , Norazmi MN , Perez Quinoy JL , Acosta A , Proteoliposomes from *Mycobacterium smegmatis* induce immune cross-reactivity against *Mycobacterium tuberculosis* antigens in mice. *Vaccine* 29(2011)6236–624.21736914
24. Garcia-Pelayo MC , Bachy VS , Kaveh DA , Hogarth PJ . BALB/c mice display more enhanced BCG vaccine induced Th1 and Th17 response than C57BL/6 mice but have equivalent protection. *Tuberculosis* 95(2015)48–53.25467292
25. Kaveh DA , Bachy VS , Hewinson RG , Hogarth PJ . Systemic BCG immunization induces persistent lung mucosal multifunctional CD4T (EM) cells which expand following virulent mycobacterial challenge. *PLoS One* 6(2011)e21566.21720558
26. Fraser JRE , Laurent TC , Laurent UBG . Hyaluronan: its nature, distribution, functions and turnover. *J. Intern. Med.* 242(1997)27–33.9260563
27. Y Yang S , O’Cearbhaill ED , Sisk GC , Park KM , K Cho W , Villiger M , Bouina BE , Pomahac B , Karp JM , Abio-inspired swellable microneedle adhesive for mechanical interlocking with tissue. *Nat. Commun.* 4(2013)1702.
28. Cao Y , Kakar P , Hossen MN , Wu MX , Chen X . Sustained epidermal powder drug delivery via skin microchannels, *J Control Release.* 249(2017)94–102.28132934
29. Wang J , Li B , Wu MX . Effective and lesion-free cutaneous influenza vaccination. *Proc. Natl. Acad. Sci. USA* 112(2015)5005–5010.25848020

30. Kleinnijenhuis J, Quintin J, Preijers F, Joosten LA, Jacobs C, Xavier RJ, van der Meer JW, van Crevel R, Netea MG, BCG-induced trained immunity in NK cells: Role for non-specific protection to infection. *Clinical Immunology*. 155(2014)213–219.25451159
31. Evans JH, Horowitz A, Mehrabi M, Wise EL, Pease JE, Riley EM, Davis DM, A distinct subset of human NK cells expressing HLA-DR expand in response to IL-2 and can aid immune responses to BCG. *Eur. J. Immunol.* 41(2011)1924–1933.21491418
32. Saunders BM, Briscoe H, Britton WJ. T cell-derived tumour necrosis factor is essential, but not sufficient, for protection against *Mycobacterium tuberculosis* infection. *Clin. Exp. Immunol.* 137(2004)279–287.15270844
33. Kozakiewicz L, Phuali J, Flynn J, Chan J. The role of B cells and humoral immunity in *Mycobacterium tuberculosis* infection. *Aiv. Exp. Med. Biol.* 783(2013)225–250.
34. Achkar JM, Casadevall A, Aitibody-mediated immunity against tuberculosis: implications for vaccine development. *Cell Host Microbe*. 13(2013)250–262.23498951
35. Leal IS, Smedegard B, Aidersen P, Appelberg R, Interleukin-6 and interleukin-12 participate in induction of a type 1 protective T-cell response during vaccination with a tuberculosis subunit vaccine. *Infect. Immun.* 67(1999)5747–5754.
36. Lin Y, Ritchea S, Logar A, Slight S, Messmer M, Rangel-Moreno J, Guglani L, Alcorn JF, Strawbridge H, Park SM, Onishi R, Nyugen N, Walter MJ, Pociask D, Randall TD, Gaffen SL, Iwakura Y, Rolls JK, A Khader S. Interleukin-17 is required for T helper 1 cell immunity and host resistance to the intracellular pathogen *Francisella tularensis*. *Immunity* 31(2009)799–810.19853481
37. Higgins SC, Jamicki AG, Lavelle EC, Mills KH, TLR4 mediates vaccine-induced protective cellular immunity to *Bordetella pertussis*: role of IL-17-producing T cells. *J. Immunol.* 177(2006)7980–7989.17114471
38. A Khader S, Gopal R, IL-17 in protective immunity to intracellular pathogens. *Virulence* 1(2010)423–427.21178483
39. van der Maaden K, Jiskoot W, Bouwstra J, Microneedle technologies for (trans) dermal drug and vaccine delivery. *J. Control. Release*. 161(2012)645–655.22342643
40. Davis SP, Martanto W, Allen MG, Prausnitz MR, Hollow metal microneedles for insulin delivery to diabetic rats. *IEEE Trans. Bio. med. Eng.* 52(2005)909–915.
41. Gardeniers HJGE, Luttge R, Berenschot EJW, Boer MJ, Yeshurun SY, Hefetz M, van't Oever R, van den Berg A, Silicon micromachined hollow microneedles for transdermal liquid transport. *J. Microelectromech. Syst.* 12(2003)855–862.
42. Gupta J, Felner EI, Prausnitz MR, Minimally invasive insulin delivery in subjects with type 1 diabetes using hollow microneedles. *Diabetes. Technol. Ther.* 11(2009)329–337.19459760
43. Mukerjee EV, Collins SD, Isseroff RR, Smith RL. Microneedle array for transdermal biological fluid extraction and in situ analysis. *Sensors Actuators APhys.* 114(2004)267–275.
44. van der Maaden K, Trietsch B, Kraan H, Varypataki EM, Romeijn S, Zwier R, van der Linden LLJ, Kersten G, Hankemeier T, Jiskoot W, Bouwstra J, Novel hollow microneedle technology for depth controlled microinjection-mediated dermal vaccination: a study with poho vaccine in rats. *Pharm. Res.* 31(2014)1846–1854.24469907
45. Quinn HL, Kearney MC, Courtenay AJ, McCrudden MT, Donnelly RF. The role of microneedles for drug and vaccine delivery. *Expert. Opin. Drug. Deliv.* 11 (2014)1769–1780.25020088
46. Cheung K, Das DB, Microneedles for drug delivery: trends and progress, *Drug, Dehv.* 25(2015)1–17.
47. Indermun S, Luttge R, Choonara YE, Kumar P, Toit LC, Modi G, Pillay V, Current advances in the fabrication of microneedles for transdermal delivery. *J. Control Release*. 185(2014)130–138.24806483
48. Matsuo K, Hirobe S, Yokota Y, Ayabe Y, Seto M, Quan YS, Kamiyama F, Tougan T, Horii T, Mukai Y, Okada N, Nakagawa S, Transcutaneous immunization using a dissolving microneedle array protects against tetanus, diphtheria, malaria, and influenza. *J. Control Release*. 160(2012)495–501.22516091

49. Morefield GL , Tammariello RF , Purcell BK , Worsham PL , Chapman J , A Smith L , Alarcon JB , A Mikszta J , Ulrich RG , An alternative approach to combination vaccines: intradermal administration of isolated components for control of anthrax, botulism, plague and staphylococcal toxic shock. *J. Immune Based Ther. Vaccines* 6(2008)5.18768085
50. García-Cuesta EM , López-Cobo S , Álvarez-Maestro M , Esteso G , Romera-Cárdenas G , Rey M , Cassidy-Cain RL , Linares A , Valés-Gómez A , Reybum HT , Martínez-Piñeiro L , Valés-Gómez M , NKG2D is a Key Receptor for Recognition of Bladder Cancer Cells by IL-2-Activated NK Cells and BCG Promotes NK Cell Activation. *Front. Immunol.* 6(2015)284.
51. Flynn JL , Chan J , Triebold KJ , K Dalton D , A Stewart T ,R Bloom B . An essential role for interferon gamma in resistance to Mycobacterium tuberculosis infection. *J. Exp. Med.* 178(1993)2249–2254.7504064
52. Mogues T , Goodrich ME , Ryan L , LaCourse R , North RJ , The relative importance of T Cell subsets in immunity and immunopathology of airborne Mycobacterium tuberculosis Infection in mice. *J. Exp. Med.* 193(2001)271–280.11157048

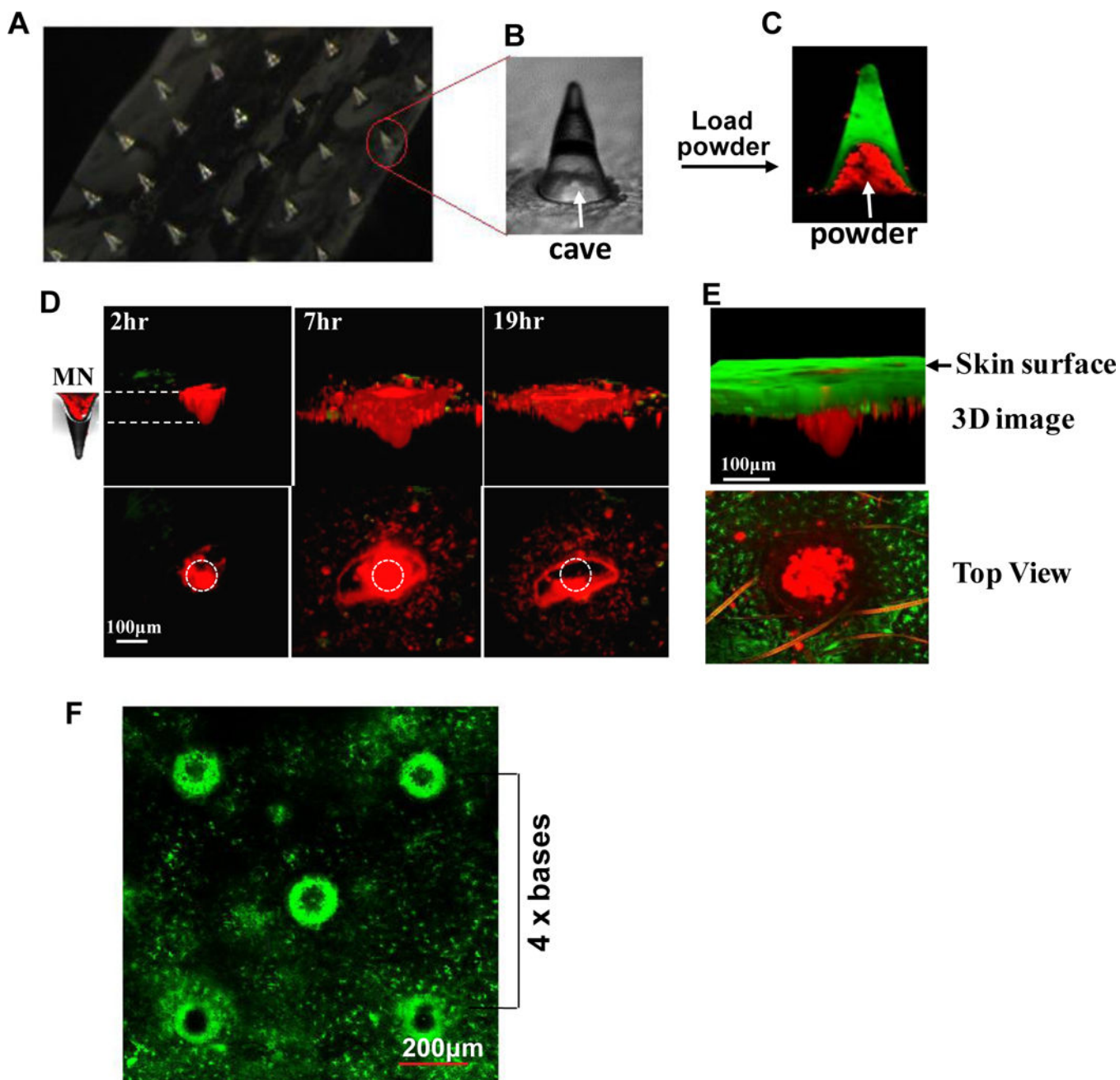


Figure 1. Dissolvable and powder-laden MNAs.

A portion of an array of dissolvable and powder-laden MNA is shown in (A). One of microneedles in A is enlarged to show the cave (B). The MNA was loaded with Alexa fluor 555-OVA powder (red), whereas FITC was embedded in shaft of the MNA (green) (C). Arrows in B&C indicate the cave in a microneedle. After insertion of the OVA-MNA into the ear of C57BL/6 mice (D) or MHC II-EGFP mice (E), OVA powder diffused into the skin over time (D). Three-D images (upper) and top views (lower) of one representative microneedle were obtained by two photon confocal microscopy at indicated times after insertion of the MNA into the skin (D). Circles in the lower panel indicate the size and

location of the microneedle. MN, microneedle. MHC II-GFP-labeled Langerhans cells in the epidermis (green) and OVA powder (red) were shown by a 3D image collected in 6 hr (upper) after OVA-MNA insertion or by a top view captured in 15 min (lower) after MNA removal (**E**). The ear of MHC II-EGFP transgenic mice was analyzed by confocal microscopy in 6 hr after removal of BCG-laden MNA (**F**). A distance between two microneedles is estimated by 4 times of the basal diameter of each microneedle (4 x bases).

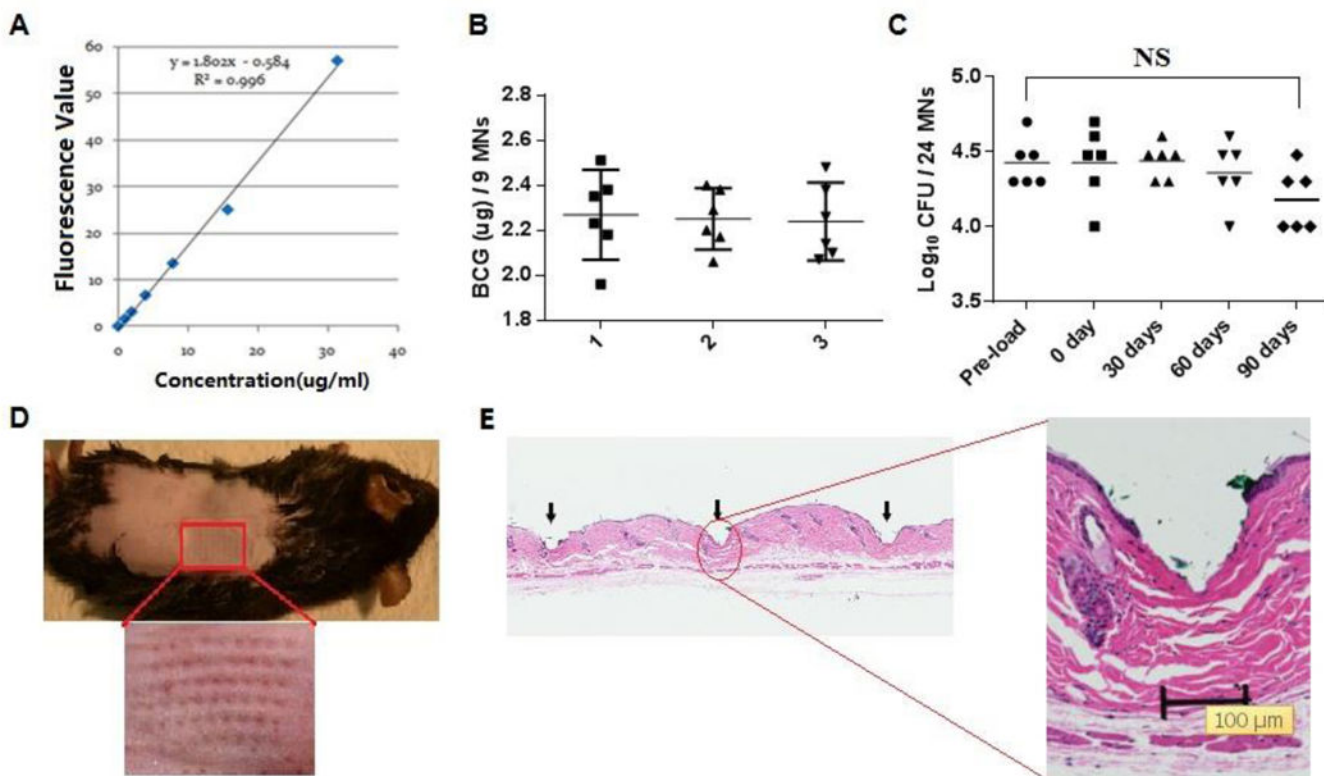


Figure 2. Characterization of BCG-MNAs.

A. A standard curve of fluorescent absorbencies at 640nm vs. varying amounts of SRB-BCG mixture. **B.** The amount of BCG powder within the MNA was evaluated in the basis of the standard curve in A. Each symbol represents the amount of BCG in nine microneedles cut from each patch and the horizontal lines are the means of 6 patches with 95% CI (confidence interval). Results of three independent experiments designated as 1, 2, and 3 were shown each with 6 MNAs and 9 microneedles in each MNA. **C.** A shelf-life of BCG-MNAs was determined on day 0, 30, 60, and 90 after MNA fabrication and storage at room temperature and compared with pre-loaded BCG vaccine. Each symbol represents the number of live bacilli or colony forming units (CFUs) per 24 microneedles and the short horizontal lines are the means of 6 patches. NS, no significant difference. Statistical significance was analyzed by ANOVA. **D.** BCG-MNA could pierce into the skin of C57BL/6 mice efficiently after 90 days of storage in room temperature, as suggested by generation of an array of micropoles in the skin with the relevant area enlarged (lower panel). **E.** Histological skin sections were prepared 2 hr after insertion of a BCG-MNA stored for 90 days in room temperature to show skin penetration of the individual microneedles (arrows), one of which is enlarged.

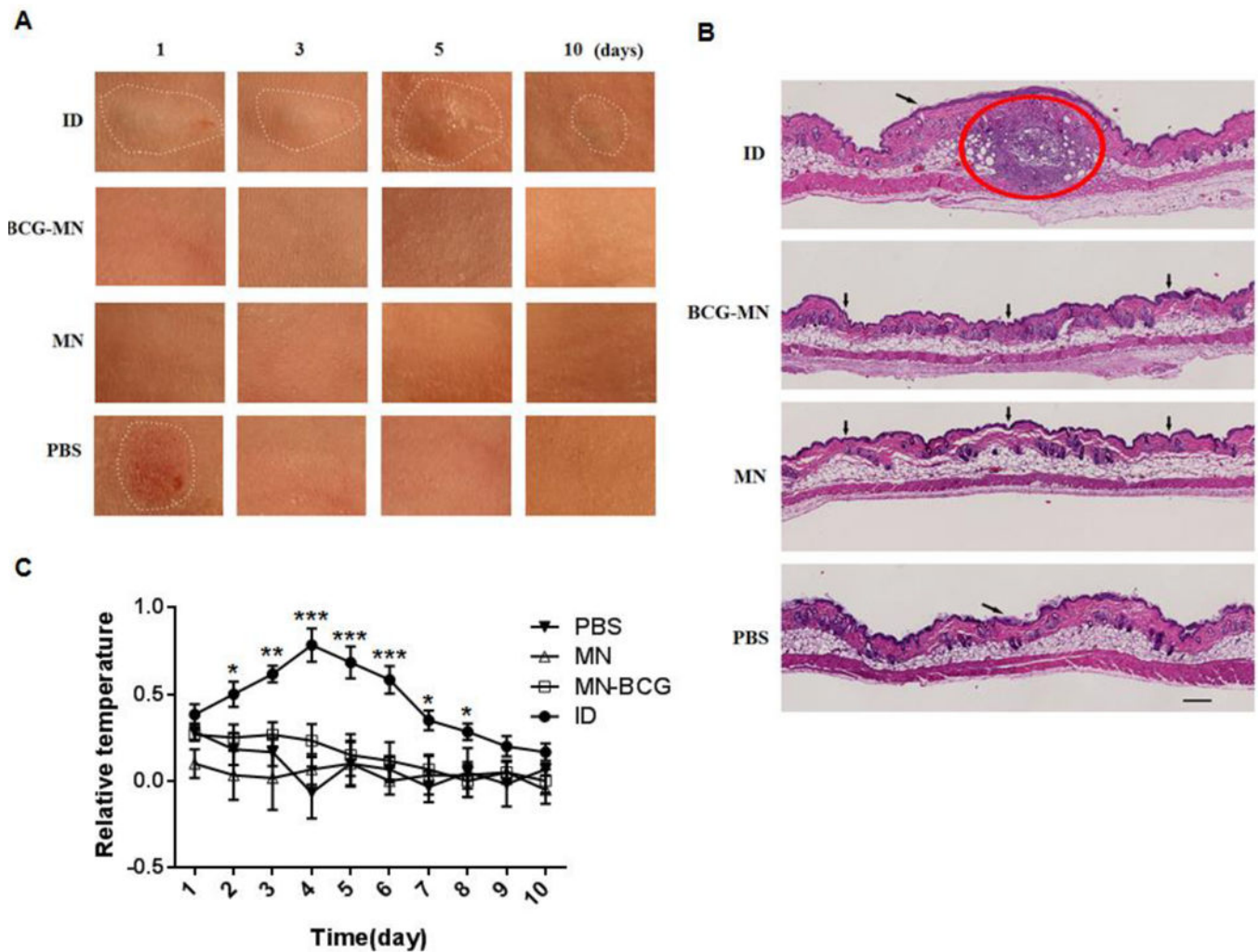


Figure 3. Reactogenicity at the site of vaccine inoculation.

A. Photos were taken in 1, 3, 5 and 10 days after inoculation. Only areas of inflammatory and abnormal skins were outlined by a white-dot line in all panels. **B.** Cross-sections of the inoculation site were H&E stained 3 days after inoculation and scanned by Nanozoomer; a red circle indicates an area of inflammation induced by BCG in the skin and arrows point the sites of a hypodermic needle or microneedle insertion. Scale bar, 200 μ m. **C.** Differences of skin surface temperature between the inoculation site and a distant area were recorded daily for 10 days (n=6). Statistical significance was analyzed by ANOVA, *P<0.05, **P<0.01, and ***P<0.001 in the presence or absence of BCG.

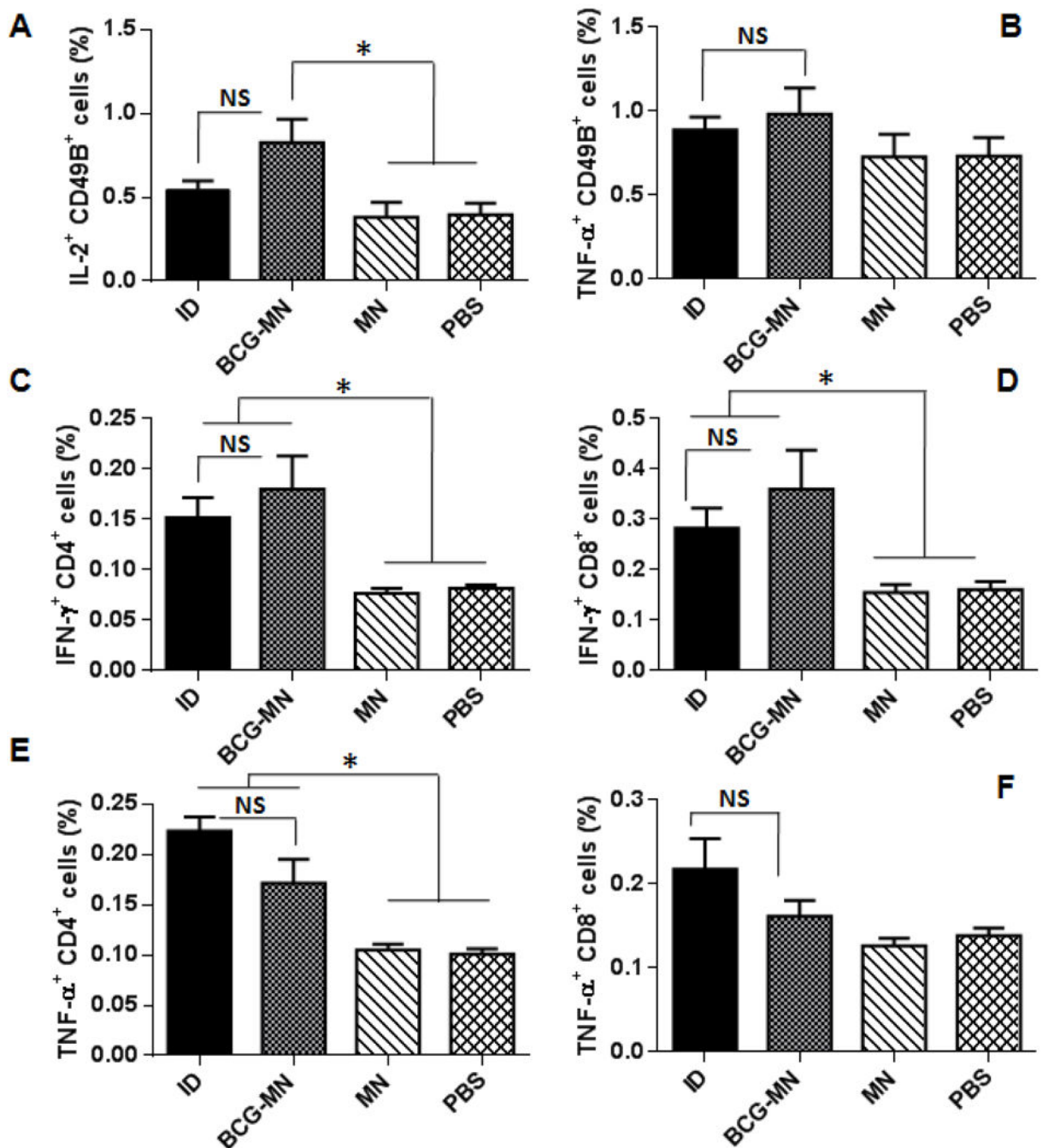


Figure 4. Intracellular cytokine productions in NK and T cells.

IL-2 (A) and TNF-α (B) production by CD49B⁺ cells were assessed in the blood samples one week after vaccination. IFN-γ⁺CD4⁺ cells (C) and IFN-γ⁺CD8⁺ cells (D), and TNF-α⁺CD4⁺ cells (E) and TNF-α⁺CD8⁺ cells (F) were analyzed in blood samples four weeks post-vaccination. Data are presented as mean±SEM (n=6). Statistical significance was analysed by ANOVA *P<0.05 and NS, no significance. All experiments were repeated twice with similar results.

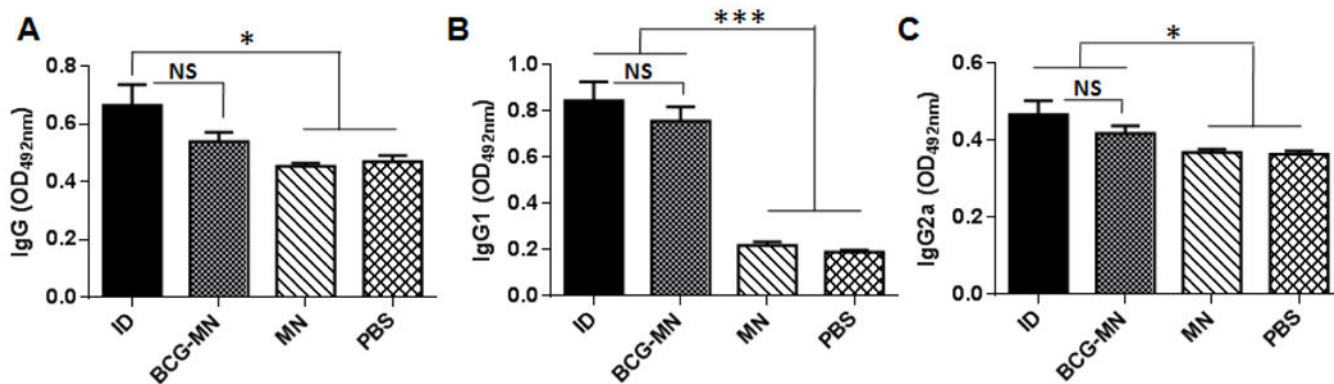


Figure 5. Similar humoral responses induced by BCG delivered via either MNA or ID. Relative IgG (A), IgG1 (B) and IgG2a (C) titers in serum were measured by ELISA 4 weeks after immunization. The data are representative of two independent studies with similar results and expressed as means \pm SEM (n =6). Statistical significance was analyzed by ANOVA (n=6 for each experiment). *P<0.05, ***P<0.001, and NS, no significance in the presence or absence of BCG.

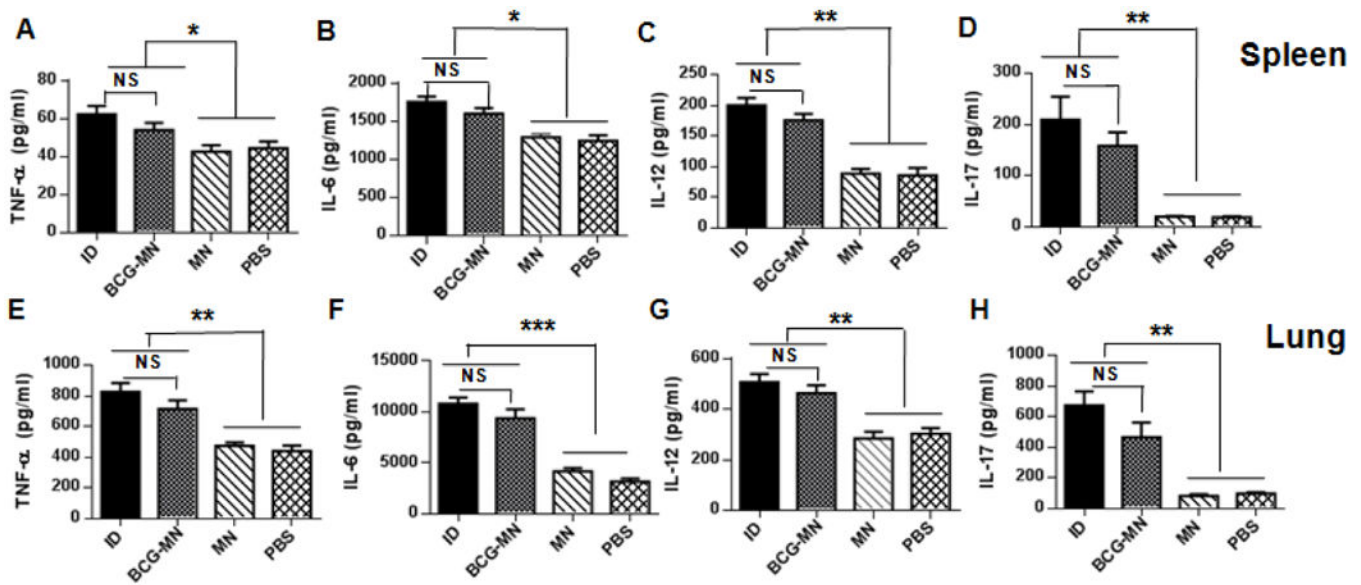


Figure 6. Representative of cytokine productions in spleen (upper) and lung (lower) after immunization.

Lymphocytes isolated from spleens (A-D) and lungs (E-H) were stimulated in vitro for 72 h with mycobacterial recombinant proteins and peptides. TNF- α , IL-6, IL-12, and IL-17 were quantified in the culture supernatants by ELISA. The data are representative of two independent studies with similar results and expressed as means \pm SEM ($n = 6$ for each experiment); * $P < 0.05$, ** $P < 0.01$, *** $P < 0.001$, and NS, no significance.